Applied Catalysis B: Environmental 147 (2014) 864–870

Contents lists available at ScienceDirect

Applied Catalysis B: Environmental

journal homepage: www.elsevier.com/locate/apcatb

Evaluation and mechanistic investigation of a AuPd alloy catalyst for the hydrocarbon selective catalytic reduction (HC-SCR) of NOx

Conor Hamill[a], Robbie Burch[a], Alex Goguet[a], David Rooney[a,*], Hafedh Driss[b], Lachezar Petrov[b], Muhammad Daous[b,**]

[a] School of Chemistry and Chemical Engineering, Queen's University Belfast, Belfast, Northern Ireland, United Kingdom
[b] Chemical and Materials Engineering Department, King Abdulaziz University, Jeddah, Saudi Arabia

ARTICLE INFO

Article history:
Received 22 July 2013
Received in revised form
19 September 2013
Accepted 28 September 2013
Available online 9 October 2013

Keywords:
Hydrocarbon SCR
NOx
Au/Pd
Mechanistic study

ABSTRACT

The ability of a gold palladium bimetallic catalyst to selectively oxidise toluene has been used to enhance the hydrocarbon selective catalytic reduction of NOx, a reaction in which the interaction of partial oxidation intermediates is considered important. The combination of gold with palladium has a synergistic effect, producing a catalyst that is more active for NOx conversion than the arithmetic sum of the corresponding mono-metallic materials. Three regimes in the conversion profile of the AuPd catalyst are proposed relating to production and consumption of toluene derived species, such as benzaldehyde and benzonitrile. The possible role of these reaction intermediates in the toluene HC-SCR reaction is examined. Using ^{15}NO, the formation of N_2 and N_2O is observed via the direct interaction between the nitrogen atom of benzonitrile and ^{15}NO. The higher activity of the bimetallic catalyst for the NOx reduction reaction by toluene is discussed in the context of these partial oxidation intermediates.

1. Introduction

Diesel engines are becoming ever more popular for automotive applications principally due to their higher fuel efficiency. However, the increasingly stringent emission legislation has created a need to develop improved after-treatment systems. Hydrocarbon Selective Catalytic reduction (HC-SCR) technology offers the potential to reduce NOx emissions using un-burnt hydrocarbon in a Compression Ignition Diesel Injection engine exhaust stream, negating the need for an external reductant such as ammonia. For the application of HC-SCR technology to become a commercially attractive competitor to the current state-of-the-art (NH_3-SCR system), HC-SCR must demonstrate activity at low temperatures and be able to operate across a wide temperature range.

Ueda et al. [1] were among the first to show the activity of highly dispersed gold based catalysts for HC-SCR, concluding that only nanoparticles less than 5 nm were active for the reaction. Seker et al. [2] showed that supporting gold on an alumina resulted in improved sulphur tolerance. Both results indicated that gold catalysts were highly selective for the formation of N_2, but were limited by their inability to activate hydrocarbons at low temperatures. Burch et al. [3] demonstrated that Pt is the most active of the PGMs at low temperatures, and that the temperature for activity increases in the order (Pt < Pd < Rh < Ir). However the use of platinum leads to very poor selectivity to N_2. Furthermore it has been demonstrated [4,5] that the presence of CO, which is readily available in an exhaust stream, can inhibit the activity of the platinum; increasing the temperatures at which such catalysts are active, as well as reducing the maximum amount of NOx that can be reduced. The reverse effect is found for Pd catalysts where CO can reduce light off temperatures and can increase the maximum amount of NOx conversion. Ueda et al. [6] showed for the H_2-SCR reaction that a TiO_2 support was more active than Al_2O_3. Further studies confirmed that this is indeed also true for the HC-SCR reaction. In addition TiO_2 [7] does not undergo the same deactivation as Al_2O_3 [8] in the presence of sulphur.

The mechanism of the HC-SCR reaction over non zeolitic catalysts has been discussed by various authors, from Burch's early NOx dissociation redox mechanism [9], to mechanisms involving the interaction of organo nitro species. In the HC-SCR reaction cyanide/nitrile (–CN) and iso-cyanate (–NCO) species are generally accepted as crucial intermediates [10]. How these species are formed is still debated with various authors proposing mechanisms involving nitro hydrocarbons, and various oximes [11,12]. However it has also been proposed that the presence of these iso-cyanate species is the result of a further reaction of the cyanide species. Furthermore it has been claimed that the presence of –NCO is a result of a cyanide 'flipping' mechanism [13], which may be heavily dependent on a metal-support interaction. Another study demonstrated

* Corresponding author. Tel.: +44 2890 974050; fax: +44 2890 974687.
** Corresponding author.
E-mail address: d.rooney@qub.ac.uk (D. Rooney).

0926-3373/$ – see front matter © 2013 Elsevier B.V. All rights reserved.
http://dx.doi.org/10.1016/j.apcatb.2013.09.047

that the rate of consumption of these iso-cyanate species was not directly related to NOx activity [14], claiming –NCO species were merely 'spectators'. Tamm et al. [11] suggested that –CN species are readily hydrolysed by water to produce amine type intermediates, which are responsible for the reduction of NO to N_2. The presence of these–NH_2 species is supported by Arve [15] who observed numerous amine species, and also concluded that these are precursors for the formation of N_2.

With respect to initial involvement of the hydrocarbon, it is widely believed that partial oxidation is an integral step in the reaction; various authors have identified the presence of aldehyde [16] and carboxylate species [17,18]. Moreover, it was demonstrated that the rate of consumption of the carboxylate species was of the same order of magnitude as that of NO to N_2 [19], thus identifying this species as a potentially important intermediate. Further to this Shibata et al. [20] proposed that this partial oxidation to produce carboxylate type species is the rate determining step in the reaction. Recently it was shown by Kesavan [21] that a gold palladium alloy can activate alkyl aromatics at low temperatures and is highly selective for the formation of oxygenated hydrocarbons. Subsequently Kesavan demonstrated experimentally that a one to one ratio (mass basis) of gold to palladium was the optimum ratio to achieve this partial oxidation. These, in combination with the knowledge that Pd/TiO_2 can provide low temperature activity, and gold can deliver high selectivities for N_2 production, would suggest that this bimetallic material may display significant potential as a HC-SCR catalyst.

A palladium and gold system was employed by Nano Stellar [22,23], for total oxidation in mobile after treatment systems. However it is noted that a Pd/Pt system was used upstream in this system as the Pd/Au system can become inhibited by the presence of hydrocarbon. Other bimetallic systems involving gold, have been used previously for HC-SCR reactions [24,25], in both instances the addition of a second metal had no significant effect on the activity. Further to this work Liu et al. [26] demonstrated a promotional effect in alloying gold with rhodium, decreasing the temperature for maximum NOx conversion to approximately 300 °C, although a significant decrease in selectivity was also observed.

The objective of the present work was first to measure the activity of $AuPd/TiO_2$ catalysts, and second to investigate the possible reaction intermediates involved and hence develop a greater understanding of the HC-SCR reaction on these catalysts using toluene as a model aromatic hydrocarbon to represent the aromatic content of a typical diesel fuel [27].

2. Experimental

2.1. Catalyst preparation

A colloidal sol of AuPd nanoparticles was generated by using reducing agents and stabiliser ligands, the latter having the role of firstly controlling the mean particle diameter range and secondly the morphology of the particles generated [28,29]. An aqueous solution of $PdCl_2$ (Sigma Aldrich) and $HAuCl_4{\cdot}3H_2O$ (Sigma Aldrich) was prepared at a 1:1 Pd:Au ratio (wt/wt). Poly vinyl alcohol (PVA) solution (1 wt%) was added to obtain a resulting ratio of PVA/(Au + Pd) (wt/wt) = 1.2. A freshly prepared solution of $NaBH_4$ (0.1 M, $NaBH_4$/(Au + Pd) (mol/mol) = 5) was then added. After 30 min of sol generation, the colloid was immobilised by adding TiO_2 (P25), (acidified to pH 1 by addition of sulphuric acid) under vigorous stirring conditions. The amount of support material required was calculated to achieve a total final metal loading of 1 wt%. After 2 h the slurry was filtered, the solid washed thoroughly with distilled water and dried at 120 °C overnight. The same method was employed when preparing catalysts with different Au:Pd ratios. A reference silver catalyst was also prepared (2 wt% Ag/Al_2O_3). In this case the necessary amount of silver nitrate (Sigma Aldrich) was impregnated onto commercially available γ-alumina (Grace-Davison). The catalyst was then dried for 3 h at 100 °C, after which the solid was calcined at 550 °C for 3 h [14].

2.2. Catalytic activity tests

Catalyst testing was performed in a quartz tube (3 mm i.d) plug flow reactor, with a typical gas composition of 720 ppm NO, 620 ppm toluene (4340 as C_1), 4.3% O_2, 7.2% H_2O, 1% Kr was used with Ar as balance and a GHSV of 60,000 ml/g/h. For isotopically labelled experiments ^{15}NO (CK gas products) was used. Products and reactants were analysed using a Hiden HPR 20 mass spectrometer in parallel with a Signal 4000 VM series NOx analyser.

2.3. Catalyst characterisation

The TEM analysis of the $Au\text{-}Pd/TiO_2$ P25 was performed using a Tecnai G2 F20 Super Twin at 200 kV with a LaB6 emitter. The microscope was fully equipped for analytical work with an energy-dispersive X-ray (EDX) detector with a S-UTW window and a high angle annular dark-field (HAADF) detector for STEM imaging. Unless stated otherwise, the scanning transmission electron microscopy (STEM) imaging and all analytical work were performed with a probe size of 1 nm resulting in a beam current of about 0.5 nA. TEM images and selected area diffraction (SAD) patterns were collected on an Eagle 2 K HR 200 kV CCD camera. The HAADF-STEM EDX and CCD line traces were collected fully automatically using the Tecnai G2 User Interface and processed with the Tecnai Imaging and Analysis (TIA) software Version 1.9.162.

3. Results and discussion

3.1. Characterisation

Fig. 1a reports the HRTEM images of $0.5Au0.5Pd/TiO_2$. The pictures obtained show the presence of highly dispersed metallic particles over the TiO_2 P25 support. This result suggests a small narrow mean particle diameter distribution has been achieved using this colloidal preparation method, which is in agreement with the findings of Hutchings et al. [21,28,29]. This result is also supported by XRD studies (Figure S1) as no Au or Pd peaks are detected. Further TEM analysis reported in Fig. 1b confirm the presence of highly dispersed nanoparticles. One particle within this image (Fig. 1c) was subjected to further EDX analysis, which demonstrated the presence of gold and palladium (Figure S2). A 2D diffractogram of this particle (Fig. 1d) shows that the structure corresponds to a cubic (1 1 1) system. Using this model and applying Vergard's Law [30] we estimated the atomic composition of this particle to be approximately 64 mol% Pd, 36 mol% Au. This result is consistent with the expected formation of bimetallic AuPd nanoparticles, which is agreement with Kesavan et al. [21]. These findings are also consistent with the Au and Pd contents as determined by Inductively Coupled Plasma Optical Emission Spectroscopy (ICP-OES) (Table S1). XPS (Figure S3) demonstrates that within the this bimetallic system both palladium and gold are in their reduced Au(0) and Pd(0) oxidation states. BET surface areas for all catalysts tested are reported in Table S2.

3.2. Catalytic experiments

The conversion of NO for the 0.5Au-0.5Pd catalyst as a function of temperature is compared to the current state-of-the art silver catalyst in Fig. 2. The 0.5Au-0.5Pd catalyst is significantly more active at low temperatures. This result is noteworthy because not

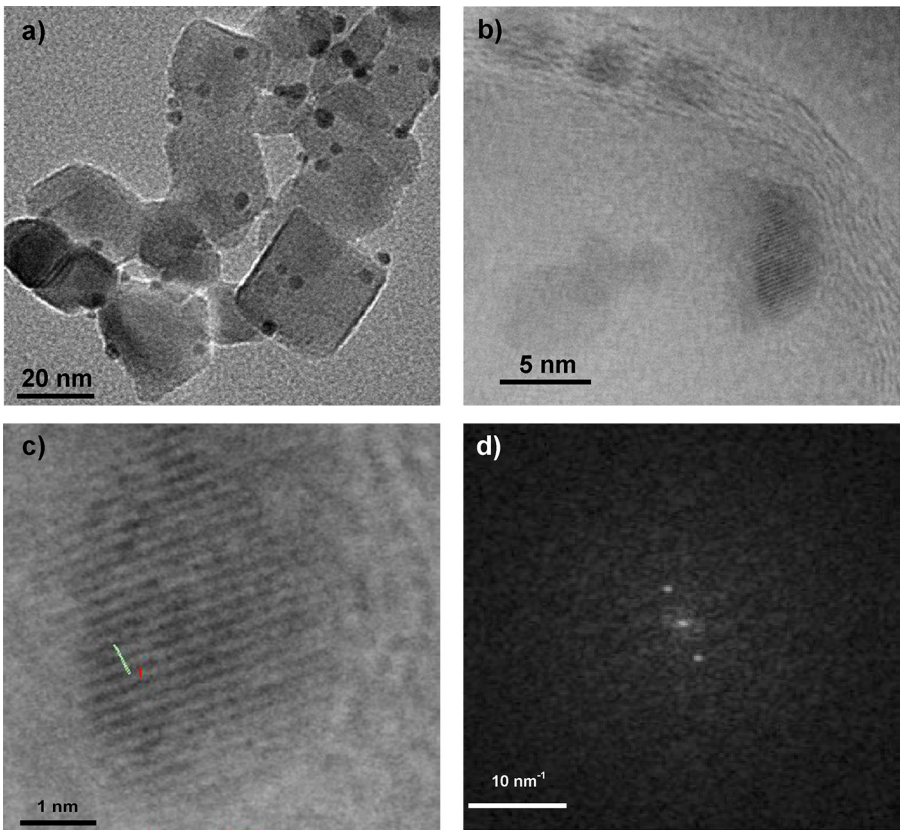

Fig. 1. HRTEM images of 0.5Au0.5Pd/TiO2 (P25) (see text for details).

only is silver a poor catalyst for the activation of toluene but also at lower temperatures toluene is a severe poison for the HC-SCR reaction with aliphatic hydrocarbons such as octane or decane [31]. The synergistic effect of combining Au and Pd is detailed in Fig. 3. As expected, Au alone is a very poor catalyst and Pd alone gives a lower maximum conversion and a significantly narrower useful temperature range than the AuPd catalyst. The Pd catalyst has a slightly sharper light-off temperature profile but the 50% conversion occurs about 40 °C sooner than for the AuPd system. The reproducibility obtained in repeat experiments is shown in Figure S4. Furthermore the catalyst was tested for 20 hours, displaying a good level of stability in the absence/presence of 5 ppm SO_2 (See Figure S5).

In an attempt to find the optimum Au/Pd ratio, a set of catalysts with varying Au/Pd compositions were compared. The results are reported in Fig. 4. It can be seen that the 0.5Au-0.5Pd catalyst still gives the highest maximum NOx conversion. However, it is interesting to note that the 0.25Au-0.75Pd catalyst has the same light-off profile as that of the Pd-only catalyst but achieves a higher maximum conversion and a much wider temperature window.

According to the results of Kesavan [21], the 1:1 (wt/wt) ratio of Au:Pd correspond to an optimum with respect to the yield of oxygenated compounds from partial oxidation of toluene. Our results would be consistent with the fact that the partial oxidation is an important step (very likely rate limiting) in the SCR and that promoting this step leads to improved overall performance.

Assuming that partial oxidation products of toluene are indeed important, it is expected that the presence of the intermediates could be observed. To investigate this possibility, an experiment

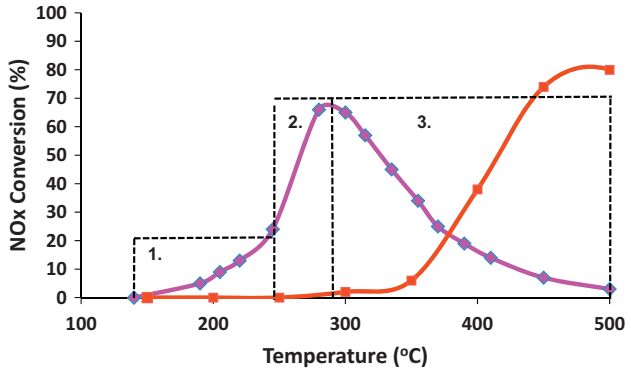

Fig. 2. The catalytic activity of 0.5 wt%Au 0.5 wt%Pd/TiO_2 (♦) as a function of temperature compared to the activity of 2% Ag/γ-Al_2O_3 (■), with three possible reaction profile regions displayed.

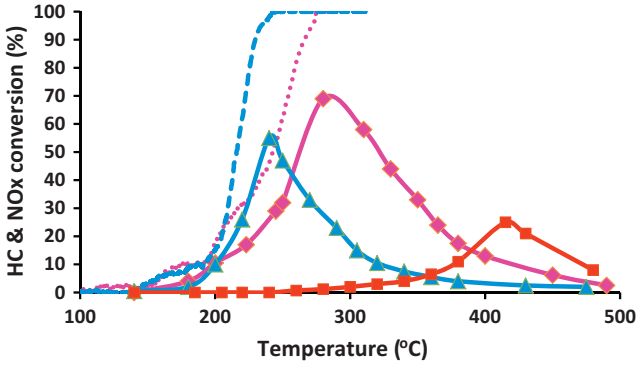

Fig. 3. The toluene and NOx (solid lines) conversion profiles as a function of temperature. 0.5 wt%Au 0.5 wt%Pd/TiO_2 (♦), 1 wt%Pd/TiO_2 (▲), 1 wt% Au/TiO_2 (■). Broken line is toluene conversion for 1 wt%Pd/TiO_2, dotted line is toluene conversion for 0.5 wt%Au0.5 wt%Pd/TiO_2.

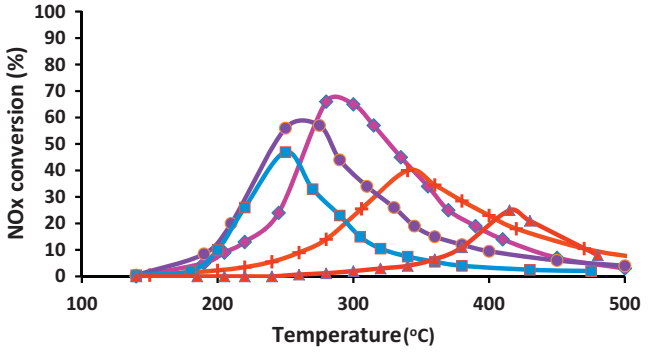

Fig. 4. The effect of Au:Pd ratio on the NOx conversion as a function of temperature. Total metal loading 1 wt% in all cases supported on TiO_2. Pd (■), 0.25Au0.7Pd (●), 0.5Au0.5Pd (♦), 0.75Au0.25Pd (+), Au (▲).

was conducted at 200 °C in which the gas stream was condensed and then analysed by GC-MS. This showed the presence of benzaldehyde and benzonitrile in an approximate ratio 40:60. It should be noted that no benzoic acid was detected.

Referring to Fig. 2, three distinct regions of the reaction profile curve can be identified as indicated by the dotted boxes. This three-part profile has been seen for several of the gold based catalysts, including those modified with various additives (Figure S6). Therefore the distinction with the profile reported for the Ag catalyst in Fig. 2, appears to be a real effect which could be related to the production and consumption of reaction intermediates.

Fig. 5 reports the result of an experiment in which various possible intermediate species were monitored as a function of temperature. The formation and reaction of benzaldehyde was observed first with subsequent formation and reaction of benzonitrile. From about 140 °C the production of benzaldehyde is observed and it increases until about 180 °C at which point the benzaldehyde either stops forming or more likely is now consumed faster than it is formed (although benzaldehyde was still detected up to about 280 °C). The formation of benzaldehyde is paralleled by the consumption of toluene which reaches a first peak at about 175 °C, plateaus briefly, and then rises steadily to reach full conversion at about 280 °C. Furthermore the formation of benzonitrile commences at about 170–180 °C and then rises steadily to a peak at about 250 °C. The increase in the benzonitrile concentration parallels quite closely the decrease in the concentration of benzaldehyde which could indicate that, as the temperature is increased, there is a reaction of benzaldehyde with NOx to form the nitrile. Above 250 °C the concentration of benzonitrile decreases as the NOx conversion increases to a peak at 280 °C which is the temperature at which all the toluene had been consumed. Pritchard et al. [32] and Tiruvalam et al. [28] demonstrate the effect of temperature on the particle size distribution of Au and Pd nanoparticles produced via Sol Immobilisation. They observed minor particle size growth at 400 °C, which

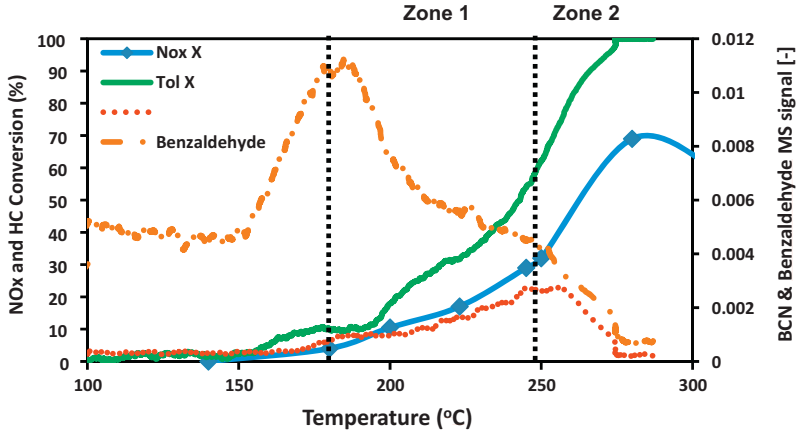

Fig. 5. The production of benzaldehyde (*m*/*z*: 105) and benzonitrile (*m*/*z*: 104) and the corresponding activities for toluene (*m*/*z*: 92) conversion and NOx reduction as a function of temperature over 0.5 wt%Au 0.5 wt%Pd/TiO_2.

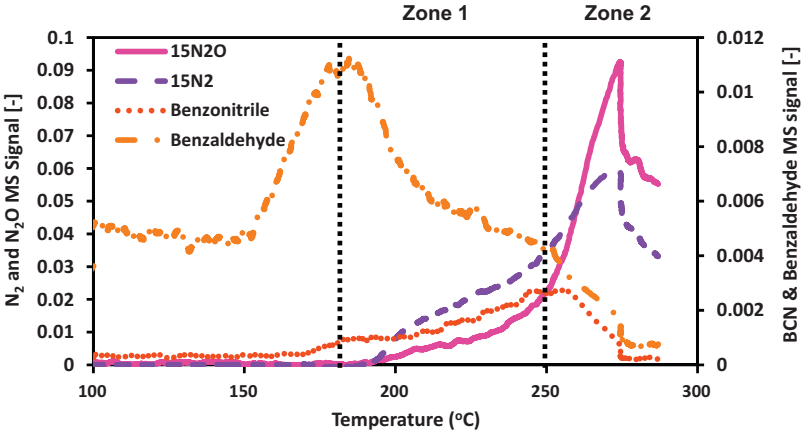

Fig. 6. Correlations between the formation of N_2 (*m*/*z*: 30) and N_2O (*m*/*z*: 46) and the production of benzaldehyde (*m*/*z*: 105) and benzonitrile (*m*/*z*: 104) as a function of temperature over 0.5 wt%Au 0.5 wt%Pd/TiO_2.

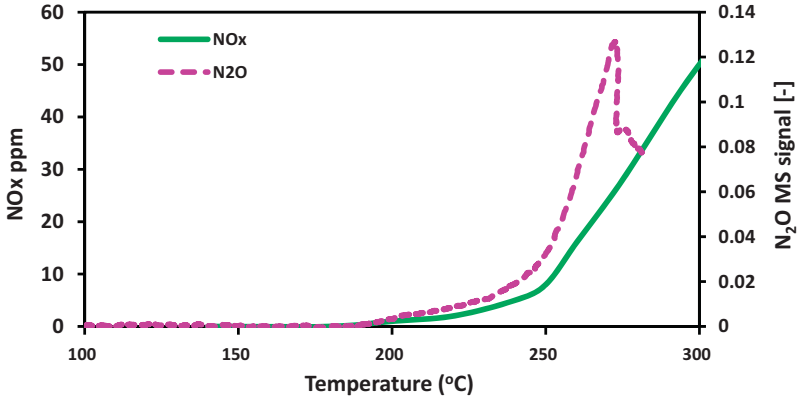

Fig. 7. Relationship between benzonitrile combustion and N_2O (m/z 45) production over 0.5 wt%Au 0.5 wt%Pd/TiO_2.

is significantly greater than the temperature for maximum deNOx activity. Furthermore Tiruvalam demonstrated that at 400 °C the particles retained their homogenously alloyed morphology.

In Fig. 5, we note again the change in slope in the NOx conversion profile and the two zones identified below and above the temperature break (250 °C). It seems possible that in zone 1 (as identified in Fig. 2) the production of benzonitrile occurs by the reaction of benzaldehyde with NO since there is some NOx conversion in this temperature range. Across zone 1, the total rate of NO removal may involve both the conversion to gaseous products (N_2 and N_2O) and the formation of adsorbed or gaseous benzonitrile. However, in zone 2 the rate of NO removal accelerates because in this temperature range the NO is both reduced by toluene and also through the parallel reaction with benzonitrile. The latter is either formed continuously or may also initially be provided from adsorbed species trapped on the catalyst surface. Of course, any adsorbed species will quickly be consumed so it is perhaps more likely that in zone 2 the higher than expected rate of reaction of NO is due to a combination of a reaction with "activated" toluene (benzaldehyde and/or benzonitrile) and also with toluene itself.

The selectivity to either N_2 or N_2O is important in the HC-SCR reaction. Fig. 6 shows the observed evolution of these products using ^{15}NO. Labelled NO was used since mass spectrometry was used to analyze the reactant and products and the AMUs for unlabelled N_2 and N_2O are 28 and 44 which are shared with CO and CO_2.

Zone 1, identified earlier as the region where benzonitrile is produced, corresponds to the initiation of N_2 and N_2O production with N_2 being the dominant product. However, in zone 2 the ratio changes and N_2O becomes the dominant species with a peak in production at about 275 °C (approximately 60% selective to N_2O). It is worth noting that there is a rapid rise in N_2O production in the region where benzonitrile is consumed. To reinforce this possible correlation between N_2O production and benzonitrile conversion we show in Fig. 7 an experiment in which benzonitrile was combusted. Remarkably, the N_2O production profile observed in Fig. 6 correlates well with the N_2O profile obtained from the combustion of benzonitrile.

To investigate whether or not benzonitrile could be formed from the reaction of benzaldehyde and NO, we passed a mixture of benzaldehyde and NO over the catalyst as a function of temperature in the presence and absence of oxygen. The results are reported in Figure S7 and demonstrate the direct formation of nitrile species from aldehyde. The results obtained in the presence of O_2, shows that the latter appears to inhibit the formation of gas phase benzonitrile, which would suggest that nitrile combustion could consequently reduce the efficiency for NOx reduction by benzaldehyde/benzonitrile.

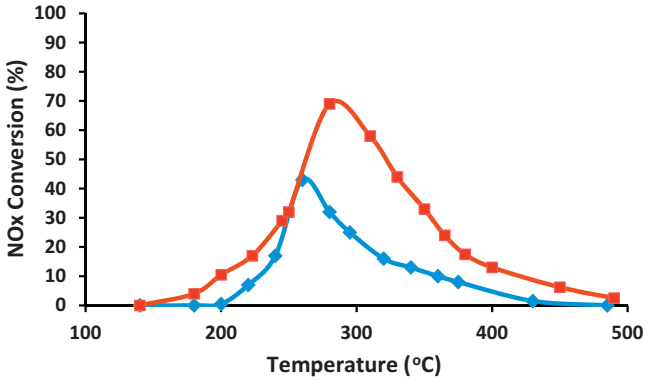

Fig. 8. NOx conversion profile when using toluene (■) or benzonitrile (♦) as the reductant over 0.5 wt%Au 0.5 wt%Pd/TiO_2.

The perceived importance of benzonitrile as a reaction intermediate was probed further by using pure benzonitrile as a reductant and comparing with toluene (Fig. 8). Clearly the benzonitrile is effective as a reductant at temperatures that are similar to those observed with toluene, supporting the suggestion that the toluene may indeed react *via* benzonitrile as an intermediate. It is recognised that the higher "conversion" of NOx at lower temperatures with toluene as the reductant is due to the trapping of some NOx as benzonitrile. This is evidenced in Fig. 6, where a delay in the production of benzonitrile and the formation of N_2 and N_2O are observed. Notice the temperature profile of benzonitrile. The acceleration in NOx conversion reported with toluene at about 250 °C is not observed in this case. This again justifies the decision to identify two separate zones in the toluene NOx reduction experiments. The significantly higher NO conversion seen with toluene at the higher temperatures may reflect the fact that benzonitrile is too easy to oxidise fully at these elevated temperatures. Note also the fact that 1 mol of toluene requires 1 mol of NO to produce the nitrile, and this nitrile then subsequently consumes another mol of NO. Therefore using toluene as the reductant will consume twice as much NOx compared to using benzonitrile.

Fig. 9 reports the product distribution using benzonitrile as the reductant for ^{15}NO in combination with ^{14}N-benzonitrile. As the benzonitrile starts to react there is a rise in the production of $^{14}N^{15}N$ which unambiguously demonstrates that the ^{14}N-benzonitrile is reacting with the ^{15}NO to produce nitrogen. As the temperature is further increased a number of other products are observed; $^{15}N^{14}NO$ is formed, likely through the reaction of ^{14}N-benzonitrile with ^{15}NO, with the oxygen presumably coming from the ^{15}NO.

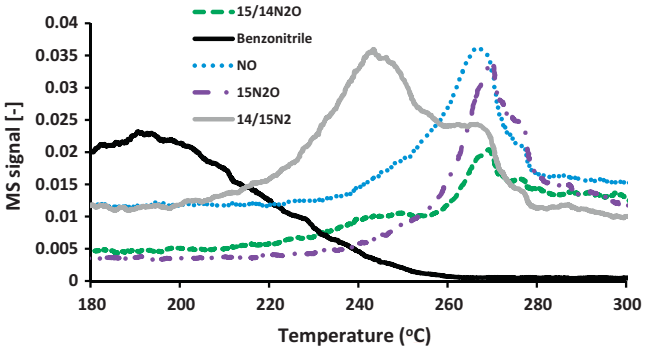

Fig. 9. The evolution/consumption of various reactants and products as a function of temperature for the reaction between ^{14}N-benzonitrileand isotopically labelled ^{15}NO over 0.5 wt%Au 0.5 wt%Pd/TiO_2. The corresponding m/z values measured were as follows: $^{14/15}N_2$ (*m*/*z*: 29), $^{14/15}N_2O$ (*m*/*z*: 45), ^{14}NO (*m*/*z*: 30), $^{15/15}N_2O$ (*m*/*z*: 46), ^{14}N-benzonitrile (*m*/*z*: 103).

The formation of $^{15}N_2O$ is also observed. This shows that there is more than one route to N_2O. It should be noted that both $^{14}NO_2$ and $^{15/15}N_2O$ share the same *m*/*z* value i.e. 46 and hence could not be unambiguously separated. Based on earlier published work [33], it is reasonable to attribute the formation of $^{15}N_2O$ to a reaction between ^{15}NO molecules on reduced (metallic) sites on the metal. Finally, it is noticeable that the "reverse" reaction whereby benzonitrile is oxidised back to NO is detected through the observation of ^{14}NO which can only come from the ^{14}N-benzonitrile (recall that we expect that benzonitrile is produced by the forward reaction of benzaldehyde with NO as seen in Figure S6).

3.3. Influence of Au on activity and selectivity of Pd/TiO_2

The reduction of NO by toluene under leanburn conditions on the 0.5Au-0.5Pd catalyst has shown that benzaldehyde and especially benzonitrile may be important intermediates in the formation of N_2 and N_2O. It is interesting, on this basis, to probe why the Au-modified catalyst is performing better than the pure Pd catalyst. As shown in Fig. 3, the conversion of toluene is delayed by the addition of Au to the Pd/TiO_2 catalyst and this inhibition of the toluene combustion matches the increase in the peak NO reduction since, for both catalysts, the maximum occurs simultaneously with the 100% conversion of the toluene.

The effect of gold on the production and reaction of benzaldehyde and benzonitrile is shown in Fig. 10. With the Pd-only catalyst, the amount of benzaldehyde detected is greater than with the Au-modified catalyst. However, the amount of benzonitrile observed

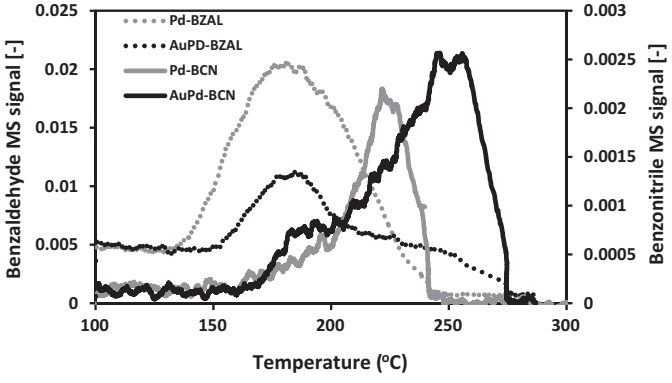

Fig. 10. Comparison of benzonitrile (*m*/*z*: 104) and benzaldehyde (*m*/*z*: 105) production over 0.5 wt%Au 0.5 wt%Pd/TiO_2 (black lines) and 1 wt%Pd/TiO_2 (blue lines).

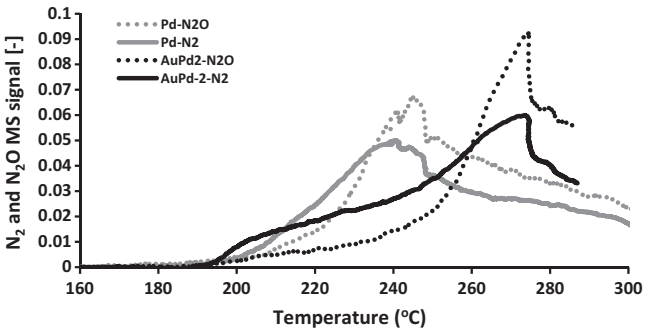

Fig. 11. Comparison of N_2 (*m*/*z*: 30) and N_2O (*m*/*z*: 46) production for 0.5 wt%Au 0.5 wt%Pd/$TiO_2$and 1 wt%Pd/TiO_2.

with the Au-modified catalyst is much greater than that observed with the Pd-only catalyst. This is particularly true in the temperature range from about 230 to 275 °C. Comparison with Fig. 3 shows that this is precisely the temperature range where the NO conversion reaches a maximum for the 0.5Au-0.5Pd catalyst. This would suggest that the addition of gold may be enhancing the reaction between benzaldehyde and NO, or may be inhibiting the combustion of benzonitrile or both.

Earlier we have linked the formation of N_2O with the presence of benzonitrile. Fig. 11 compares the selectivities of the Au-modified and the Pd-only catalysts. The Pd-only catalyst, which is a better combustion catalyst, produces more N_2O at lower temperatures than the Au-modified catalyst but less N_2O at the higher temperatures. We also note that the shift in the peak temperatures for N_2O formation (see Fig. 11) is approximately 30 °C which is quite close to the shift of the peak temperatures for the amount of benzonitrile detected (see Fig. 10).

The set of results shown in Figs. S8–S10 further support the correlations between benzonitrile formation and both the overall NO reduction activity and the selectivity to N_2O. Fig. S8 shows that when a small amount of CO (1000 ppm) is added to the reaction mixture, the NOx conversion is greatly diminished. This is reflected (see Fig. S9) in a greatly reduced production of benzaldehyde and especially benzonitrile. Finally, the production of N_2O (see Fig. S10) is also greatly reduced when CO is present which matches the lower amount of benzonitrile. These observations are consistent with our earlier hypothesis that the formation of benzonitrile is correlated with the NOx conversion and the selectivity to N_2O.

4. Conclusions

It has been observed that there is a synergetic effect of alloying Au with Pd. Furthermore we have observed the interaction of partially oxygenated species with NO to produce gas phase benzonitrile. The direct interaction of this nitrile with NO has been shown to lead to the formation of N_2 and N_2O. Analysis of the results suggests that there may be two competing parallel reaction pathways for the consumption of these –CN species, both of which are critical in dictating the selectivity of a catalyst towards N_2 production. The nitrile may be readily reduced by NO to produce N_2, or it may be further oxidised leading to formation of N_2O. It has been demonstrated that a catalyst with better combustion activity is more selective to N_2O production. Due to the high levels of N_2O production, along with the various other gas phase species present, the 0.5 wt%Au0.5 wt%Pd catalyst is considered unsuitable for commercial application. However it may be possible to utilise the findings of this study to develop a catalyst that allows functional control over both the rates of these parallel reactions, yielding a more selective low temperature HC-SCR catalyst.

Acknowledgments

This work was supported by the Deanship of Scientific Research, King Abdulaziz University, Jeddah, Saudi Arabia under grant No. (D-005/431), and the Department of Employment and Learning, Northern Ireland.

Appendix A. Supplementary data

Supplementary data associated with this article can be found, in the online version, at http://dx.doi.org/10.1016/j.apcatb.2013.09.047.

References

[1] A. Ueda, T. Oshima, M. Haruta, Appl. Catal. B-Environ. 12 (1997) 81–93, http://dx.doi.org/10.1016/S0926-3373(96)00069-0.
[2] E. Seker, E. Gulari, Appl. Catal. A-Gen. 232 (2002) 203–217, http://dx.doi.org/10.1016/S0926-860X(02)00115-1.
[3] R. Burch, M.D. Coleman, Appl. Catal. B: Environ. 23 (1999) 115–121, http://dx.doi.org/10.1016/S0926-3373(99)00073-9.
[4] A. Abu-Jrai, A. Tsolakis, Int. J. Hydrogen Energy 32 (2007) 2073–2080, http://dx.doi.org/10.1016/j.ijhydene.2006.10.003.
[5] N. Macleod, R.M. Lambert, Appl. Catal. B: Environ. 35 (2002) 269–279, http://dx.doi.org/10.1016/S0926-3373(01)00264-8.
[6] A. Ueda, T. Nakao, M. Azuma, T. Kobayashi, Chem. Lett. (1998) 595–596, http://dx.doi.org/10.1246/cl.1998.595.
[7] Z. Zhang, M. Chen, Z. Jiang, W. Shangguan, J. Environ. Sci. 22 (2010) 1441–1446, http://dx.doi.org/10.1016/S1001-0742(09)60273-4.
[8] F.C. Meunier, J.R.H. Ross, Appl. Catal. B: Environ. 24 (2000) 23–32, http://dx.doi.org/10.1016/S0926-3373(99)00088-0.
[9] R. Burch, P.J. Millington, A.P. Walker, Appl. Catal. B: Environ. 4 (1994) 65–94, http://dx.doi.org/10.1016/0926-3373(94)00014-X.
[10] N. Bion, J. Saussey, M. Haneda, M. Daturi, J. Catal. 217 (2003) 47–58, http://dx.doi.org/10.1016/S0021-9517(03)00035-6.
[11] S. Tamm, H.H. Ingelsten, A.E.C. Palmqvist, J. Catal. 255 (2008) 304–312, http://dx.doi.org/10.1016/j.jcat.2008.02.019.
[12] E. Joubert, X. Courtois, P. Marecot, C. Canaff, D. Duprez, J. Catal. 243 (2006) 252–262, http://dx.doi.org/10.1016/j.jcat.2006.07.018.
[13] F. Thibault-Starzyk, E. Seguin, S. Thomas, M. Daturi, H. Arnolds, D.A. King, Science 324 (2009) 1048–1051, http://dx.doi.org/10.1126/science.1169041.
[14] S. Chansai, R. Burch, C. Hardacre, J. Breen, F. Meunier, J. Catal. 281 (2011) 98–105, http://dx.doi.org/10.1016/j.jcat.2011.04.006.
[15] K. Arve, H. Backman, F. Klingstedt, K. Eränen, D.Y. Murzin, Appl. Catal. B: Environ. 70 (2007) 65–72, http://dx.doi.org/10.1016/j.apcatb.2005.10.036.
[16] Y.H. Yeom, M. Li, W.M.H. Sachtler, E. Weitz, J. Catal. 246 (2007) 413–427, http://dx.doi.org/10.1016/j.jcat.2006.12.013.
[17] K. Shimizu, A. Satsuma, Phys. Chem. Chem. Phys. 8 (2006) 2677–2695, http://dx.doi.org/10.1039/b601794k.
[18] K. Shimizu, J. Shibata, H. Yoshida, A. Satsuma, T. Hattori, Appl. Catal. B: Environ. 30 (2001) 151–162, http://dx.doi.org/10.1016/S0926-3373(00)00229-0.
[19] K. Shimizu, H. Kawabata, A. Satsuma, T. Hattori, J. Phys. Chem. 103 (1999) 5240–5245, http://dx.doi.org/10.1021/jp984770x.
[20] J. Shibata, K. Shimizu, S. Satokawa, A. Satsuma, T. Hattori, Phys. Chem. Chem. Phys. 5 (2003) 2154–2160.
[21] L. Kesavan, R. Tiruvalam, M.H.A. Rahim, M.I. bin Saiman, D.I. Enache, R.L. Jenkins, N. Dimitratos, J.A. Lopez-Sanchez, S.H. Taylor, D.W. Knight, C.J. Kiely, G.J. Hutchings, Science 331 (2011) 195–199, http://dx.doi.org/10.1126/science.1198458.
[22] K. Fujdala, T. Truex, J. Jia, Nanostellar Inc., Engine Exhaust Catalysts Containing Pd-Au. 7,745,367 B2 (2009).
[23] M. Peplow, Nature 495 (2013) S10–S11.
[24] C. Mihut, B. Chandler, M. Amiridis, Catal. Commun. 3 (2002) 91–97, http://dx.doi.org/10.1016/S1566-7367(02)00055-9.
[25] K. Arve, J. Adam, O. Simakova, L. Capek, K. Eranen, D.Y. Murzin, Topics in Catalysis 52 (2009) 1762–1765, http://dx.doi.org/10.1007/s11244-009-9338-6.
[26] L. Liu, X. Guan, Z. Li, X. Zi, H. Dai, H. He, Appl. Catal. B: Environ. 90 (2009) 1–9, http://dx.doi.org/10.1016/j.apcatb.2009.02.022.
[27] J.P. Breen, R. Burch, C. Hardacre, C.J. Hill, B. Krutzsch, B. Bandl-Konrad, E. Jobson, L. Cider, P.G. Blakeman, L.J. Peace, M.V. Twigg, M. Preis, M. Gottschling, Appl. Catal. B: Environ. 70 (2007) 36–44, http://dx.doi.org/10.1016/j.apcatb.2006.05.005.
[28] R.C. Tiruvalam, J.C. Pritchard, N. Dimitratos, J.A. Lopez-Sanchez, J.K. Edwards, A.F. Carley, G.J. Hutchings, C.J. Kiely, Faraday Discuss 152 (2011) 63–86, http://dx.doi.org/10.1039/c1fd00020a.
[29] J. Pritchard, L. Kesavan, M. Piccinini, Q. He, R. Tiruvalam, N. Dimitratos, J. Lopez-Sanchez, A.F. Carley, J.K. Edwards, C.J. Kiely, G.J. Hutchings, Langmuir 26 (2010) 16568–16577, http://dx.doi.org/10.1021/la101597q.
[30] H. Okamoto, T.B. Massalski, Bull. Alloy Phase Diagrams 6 (1985) 229–235, http://dx.doi.org/10.1007/BF02880404.
[31] V. Demidyuk, C. Hardacre, R. Burch, A. Mhadeshwar, D. Norton, D. Hancu, Catal. Today 164 (2011) 515–519, http://dx.doi.org/10.1016/j.cattod.2010.12.047.
[32] J. Pritchard, M. Piccinini, R. Tiruvalam, Q. He, N. Dimitratos, J.A. Lopez-Sanchez, D.J. Morgan, A.F. Carley, J.K. Edwards, C.J. Kiely, G.J. Hutchings, Catal. Sci. Technol. 3 (2013) 308–317, http://dx.doi.org/10.1039/c2cy20234d.
[33] R. Burch, A.A. Shestov, J.A. Sullivan, J. Catal. 188 (1999) 69–82, http://dx.doi.org/10.1006/jcat.1999.2653.